Colloid Polym Sci 274:989–994 (1996)

SHORT COMMUNICATION

F. Aliotta
V. Arcoleo
G. La Manna
V. Turco Liveri

Structural and dynamical investigation of gelatin containing water-in-oil microemulsions

Received: 20 October 1995
Accepted: 23 January 1996

F. Aliotta
Istituto di Tecniche Spettroscopiche
del C.N.R.
Salita Sperone 31
98166 Messina, Italy

V. Arcoleo · G. La Manna
Prof. V. Turco Liveri (✉)
Dipartimento di Chimica-Fisica
Università Palermo
Via Archirafi 26
90123 Palermo, Italy

Abstract The gelatin (Bloom 300)/water/AOT/*n*-heptane system has been investigated at fixed water/AOT molar ratio R ($R = 31.1$) as a function of the gelatin content. Several experimental techniques (densitometry, refractometry, conductometry, rheology, dielectrometry, ultrasonics, hypersonics) have been used to investigate the role played by the gelatin molecule in the observed sol–gel transition above a critical gelatin content. The results appear consistent with the hypothesis of a rigid network of gelatin–water rods coated by surfactant molecules coexisting with gelatin-free AOT reversed micelles at the gelation point.

Key words Gelatin – water-in-oil microemulsions – sol–gel transition

Introduction

Water-in-oil microemulsions are made up of nanodroplets of water, coated by a monomolecular layer of surfactant molecules and dispersed in an oil-rich continuous phase. It is well known that, by increasing the volume fraction, ϕ_v, of the dispersed phase (water plus surfactant) above system dependent threshold values, a noticeable increase of some transport parameters (viscosity, conductivity, permittivity) of these systems is observed [1, 2]. In particular, in the case of water/AOT/hydrocarbon systems, such a behavior was interpreted in terms of percolative phenomena [3–5]: the hopping mechanism of surfactant anions or molecules among neighboring micelles promotes the formation of large local aggregates of micelles that, under suitable conditions, can grow dramatically giving rise to an infinite dynamical cluster of reversed micelles.

Recently, it was observed that when some hydrophilic molecules, such as gelatin are solubilized in the water pools of unpercolated microemulsions the formation of clear and optically isotropic gel is promoted. The sol–gel transition takes place above a threshold value of the solubilizate concentration [6, 7]. We have to expect that both structural and dynamical properties of these gels strongly differ from those of percolated water/AOT/hydrocarbon microemulsions. In fact, if one takes into account that the averaged molecular weight of gelatin is about 10^5 gmol^{-1} (corresponding to an apparent volume of $1.2 \cdot 10^5$ Å^3) and the gelatin gyration radius [8] is about 170 Å, it should be realized that the gelatin size is comparable with the size of the aqueous core of the AOT reversed micelles (as an example, at $R = 30$ the volume and the radius of the aqueous core are $6.6 \cdot 10^5$ Å^3 and 54 Å, respectively) [9]. It follows that gelatin solubilization within AOT reversed micelles involves significant changes of the micellar volume and shape. Besides, the experimental observation of a gelatin process means that gelatin strongly affects intermicellar interactions.

In summary, from the whole body of the experimental results [7, 10] the following picture can be drawn:

i) gelatin is confined within hydrophilic nanodomains since it is practically insoluble in the oil phase

ii) we can look at these gelatin containing nano-domains as rather dense nanogels since, just below the gelation point, the concentration of the gelatin with respect to the water content of the system is very high

iii) these nano-domains show a tendency to aggregation which is stronger than that of gelatin-free AOT reversed micelles.

The above picture is consistent with the results of a recent small-angle neutron scattering experiment [11] that indicate a clear change in the microstructure of the system at the gelation point. Such a change was interpreted in terms of the formation of an extensive network of rigid rods of water and gelatin surrounded by a shell of surfactant.

In spite of all this knowledge, the structural and dynamical properties of these nanogels are, up to now, not well defined. With this in mind, we tried to add some light on the structural and dynamical properties of the system by investigating its volumetric, refractometric, conductometric, rheological, dielectric, ultrasonic and hypersonic properties. In particular, we tried to obtain new information about the relaxation processes taking place in the system, triggered by the presence of the macromolecule. These data allowed us to show how the system evolution, as the gelatin content increases, can be interpreted in terms of a continuous modification from an ensemble of weakly interacting aggregates towards a situation in which the establishment of very strong interactive forces drives the building up of the infinite connectivity characterizing the gel structure.

Experimental section

Sodium bis (2-ethylhexyl) sulfosuccinate, AOT, (Sigma 99%) was purified and dried following a procedure described elsewhere [12]. *N*-heptane (Sigma product, 99.5% stated purity) was used as received. Gelatin (Bloom 300, Sigma) was used without additional purification. The water was a deionized and bidistilled laboratory supply. Because of an intramolecular gelatin folding process, freshly prepared gelatin containing microemulsions show, at least initially, time-dependent physico–chemical properties. As a consequence, the measurements were performed at least 3 days after the sample preparation.

All the microemulsions were prepared by weight. A water/AOT/*n*-heptane microemulsion was prepared with an AOT molal concentration 0.6512 mol·Kg^{-1} and a molar ratio $R = 31.1$. Then gelatin was added in order to obtain samples at different gelatin concentration.

The densities, ρ, of the samples were determined by a vibrating tube flow densimeter (A. Paar, DMA 60/601) with an uncertainty of 3 ppm. The densimeter was calibrated with vacuum and pure water.

Refractive indices, n, were measured by a Pulfrich refractometer (Hilgher and Watt) with a V block thermostated within $\pm$ 0.02 °C. A sodium lamp ($\lambda = 589.59$ nm) was used as a light source. The uncertainty in n was $\pm$ 0.00005.

The viscosities, η, at 25 $\pm$ 0.01 °C were measured with Ubbelohde micro-viscometers, equipped with an automatic viscosity measuring unit, AVS 440 from Schott. Care was taken in choosing micro-viscometers with sufficient long flow-through time ($t > 100$ s) to minimize the kinetic energy corrections. The calibration procedure was reported elsewhere [13].

Conductances, σ, were measured by an a.c. bridge, similar to that described by Janz-McIntyre, provided with a frequency range of 1, 2, 5 and 10 KHz which enables polarization correction. A flux cell (cell constant 0.4510 $\pm$ 0.0002 cm^{-1} at 25 °C) with bright platinum electrodes was used. The temperature of the cell was regulated by an oil bath within $\pm$ 0.005 °C. Solvent conductance correction was also applied.

The *n*-heptane density and refractive index were found to be 0.67965 g·cm^{-3} and 1.38512 respectively, in fair agreement with literature values [14, 15]. Experimental densities, refractive indices, viscosities and conductivities as function of the overall gelatin weight percent (%gel, w/w) are reported in Table 1.

The dielectric measurements were performed, in the frequency range 0.1/25 GHz, by means of a high resolution communications signal analyzer (CSA 803, Tektronix) equipped with a dual-channel 17.5 ps raise time sampling head (SD-24 TDR/Sampling head, Tektronix) using an experimental procedure described elsewhere [16]. In Fig. 1, we report the real part of the complex permittivity, ε', for some samples at different gelatin content as a function of the frequency (ν). All the dielectric spectra are

Table 1 Densities, refractive indices, viscosities and conductivities of gelatin containing water/AOT/*n*-heptane microemulsions at various gelatin concentrations

% Gel overall	ρ (g·cm^{-3})	n	η (cP)	$\sigma \cdot 10^5$ (Ω^{-1}·m^{-1})
0.000	0.79232	1.3864	1.589	1.20
0.792	0.79508	1.3872	2.317	1.11
2.533	0.80091	1.3887	3.853	1.11
3.864	0.80537	1.3901	5.048	1.09
7.390	0.81714	1.3942	11.10	1.32
8.578	0.82120	1.3957	26.19	2.48
9.515	0.82453	1.3964	69.20	7.87
11.35	0.83041	1.3976	326.2	65.6
12.44	0.83404	1.3983	–	–

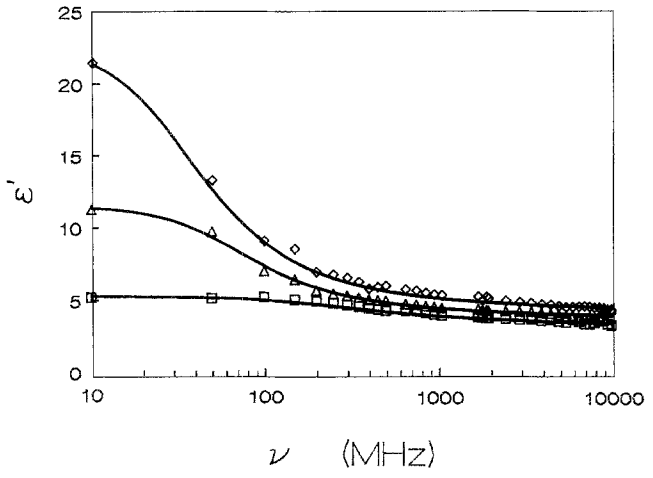

Fig. 1 Real part of the complex permittivity, ε', of water/AOT/*n*-heptane microemulsions as a function of the frequency. Data at 25 °C are reported for different gelatin contents: gelatin free microemulsions (squares), 2.5% (triangles), 12.4% (rhombuses). Continuous lines represent the fitting results with Eq. (2)

Table 2 Dielectric parameters of gelatin containing water/AOT/*n*-heptane microemulsions as a function of gelatin concentration at fixed AOT molal concentration ($m_{AOT} = 0.6512\,\text{mol}\cdot\text{Kg}^{-1}$) and at 25 °C

% Gel overall	ε_0	$\varepsilon_0-\varepsilon_\infty$	τ (ps)	β
0.000	5.2	1.91	670	0.46
0.792	8.2	4.12	1240	0.72
2.533	11.5	7.44	2950	0.68
3.864	14.0	9.10	3600	0.50
7.390	17.4	13.50	5100	0.50
9.515	18.4	14.35	5340	0.55
11.35	20.8	16.50	5500	0.55
12.44	22.5	18.02	5720	0.66

well fitted, in the 0.1/10 GHz frequency range, with a Davidson–Cole dispersion law:

$$\varepsilon = \varepsilon_\infty + \frac{\varepsilon_0 - \varepsilon_\infty}{(1 + i\omega\tau)^\beta} - \frac{i\sigma}{\varepsilon_V \omega}, \tag{1}$$

where ε_∞ is the permittivity at "infinite" frequency, $\varepsilon_0 - \varepsilon_\infty$ is the dielectric relaxation amplitude, ε_V is the vacuum absolute permittivity ($\varepsilon_V = 8.854 \cdot 10^{-12}$ F/m), ω the angular frequency, σ the static conductivity, τ the mean relaxation time and β the width of the distribution of the relaxation times. Continuous lines in Fig. 1 represent the fitting results of ε' with the real part of Eq. (1):

$$\varepsilon' = \varepsilon_\infty + \frac{\varepsilon_0 - \varepsilon_\infty}{\sqrt{(1 + \omega^2\tau^2)^\beta}} \cos[\beta \cdot \tan^{-1}(\omega\tau)]\,. \tag{2}$$

In Table 2, we summarize the results from the fitting procedure.

The ultrasonic measurements were performed by means of a Matec pulse echo analyzer in the frequency range 2/130 MHz at the temperatures of 15°, 25° and 35 °C.

The Brillouin scattering measurements were performed by means of a double pass Fabry–Perot interferometer, working at a free spectral range of 10.5 GHz, using the 5145 Å line of an Ar^+ laser (Spectra-Physics 171, with intracavity etalon) at a mean power of 0.5 W. The measurements were performed at fixed temperature ($T = 25$ °C) using a VV scattering geometry. The samples were investigated at different scattering angles ($30° \le \theta \le 150°$) corresponding to an exchanged wave vector (k) range $8.7 \cdot 10^4/3.3 \cdot 10^5\ \text{cm}^{-1}$. The experimental spectra were analyzed by fitting them to the usual expression [17]

$$I_{VV}(\omega) = \frac{A_R\Gamma_R}{\omega^2 + \Gamma_R^2} + \left[\frac{A_B\Gamma_B}{[\omega - (\omega_B^2 - \Gamma_B^2)^{1/2}]^2 + \Gamma_B^2} + \frac{A_B\Gamma_B}{[\omega + (\omega_B^2 - \Gamma_B^2)^{1/2}]^2 + \Gamma_B^2}\right]$$
$$+ \frac{\Gamma_B}{\omega_B^2 + \Gamma_B^2} \cdot \left[\frac{\omega - (\omega_B^2 - \Gamma_B^2)^{1/2}}{[\omega - (\omega_B^2 - \Gamma_B^2)^{1/2}]^2 + \Gamma_B^2} + \frac{\omega + (\omega_B^2 - \Gamma_B^2)^{1/2}}{[\omega + (\omega_B^2 - \Gamma_B^2)^{1/2}]^2 + \Gamma_B^2}\right] \tag{3}$$

where the symbols have the usual meanings. The fitting furnishes the values of the relevant parameters, namely, the frequency shift ω_B and the HWHM Γ_B of the Brillouin lines from which the values of the hypersonic velocity, $v_h = \omega_B/k$, and of the normalized absorption, $\alpha/\nu^2 = 2\pi\Gamma_B/(v_h\omega_B^2)$ are easily obtained.

Results and discussions

Assuming an additive rule for the density and the refractive index, we extracted the micellar contribution according to the expression:

$$\rho_{mic} = \frac{\rho - (1 - \phi)\rho_{hept}}{\phi}, \qquad n_{mic} = \frac{n - (1 - \phi)n_{hept}}{\phi}.$$

The dependence of the micellar density and the refractive index upon the volume fraction of the dispersed phase is reported in Fig. 2. The data exhibit a clear change in the

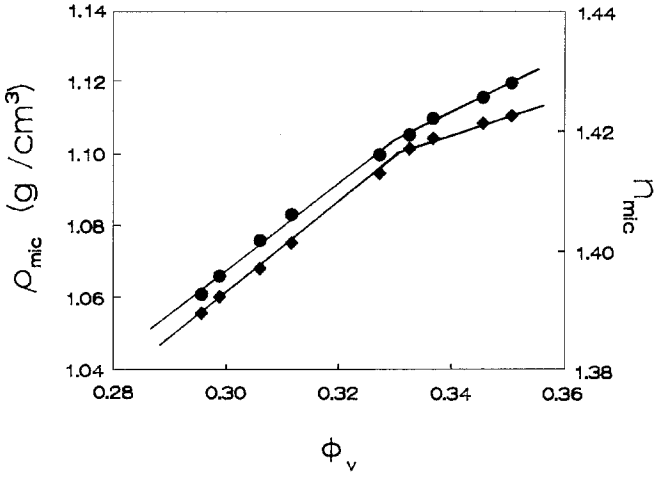

Fig. 2 Dependence of the micellar density (circles) and refractive index (rhombuses) upon the volume fraction of the dispersed phase at 25 °C

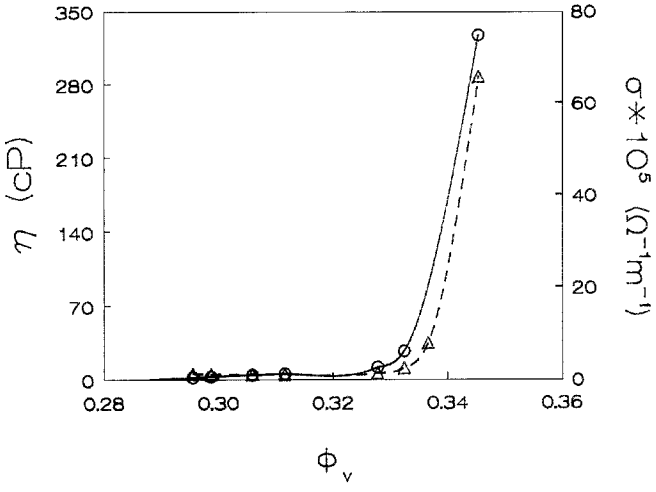

Fig. 3 Dependence of the viscosity (circles) and electrical conductivity (triangles) upon the volume fraction of the dispersed phase at 25 °C. The lines are guides for eye

slope at $\phi_V^* \cong 0.33$. The observed occurrence of two distinct regimes suggests that, at this value of the concentration, some structural change is taking place in the system. In particular, the lower slope of the data at $\phi_V \geq \phi_V^*$ could be an indication of the building up of some lower density structure when the gelatin content reaches a threshold value.

In Fig. 3, we report the viscosity and electrical conductivity of gelatin containing water/AOT/*n*-heptane microemulsions as a function of the volume fraction of the dispersed phase, at $T = 25$ °C. As can be seen, both these data show abruptly diverging behavior above the same value of the volume fraction ($\phi_V^* \cong 0.33$). It is quite evident that we are observing the same threshold of a structural transition indicated by the density and the refractive index data. It is to be stressed that viscosity evolves, below the structural transition, with a scaling law whose exponent is larger than that typical of gelatin-free micelles [18]. It follows that the presence of gelatin molecules increases the stickiness of the micelles. The same suggestion came from the comparison of the ϕ_V^* value for our samples with that observed in gelatin-free microemulsion ($\phi_V^* = 0.52$) [18]. Furthermore, it is to be noticed that the structural transition takes place at a gelatin content ($\cong 7.39\%$ by weight) which is far higher than the gelatin concentration necessary to observe the sol–gel transition in the gelatin/water system (0.54% by weight) [8]. This later consideration suggests that, in microemulsions, gelatin molecules are coated by an oriented layer of surfactant molecules. Such a structural hypothesis, implying a drastic lowering of the cross-link probability, could furnish an explanation of the experimental results.

In Fig. 4, we report the ϕ_V-dependence of the relaxation time and of the permittivity at zero frequency, as obtained from the dielectric measurements. We observe that, below the cross-over concentration, an increasing of the gelatin content enhances the observed process while the exchange rate is lowered (ε_0 and τ increase). Assuming that the observed relaxation process is to be connected with some exchange process of AOT ions among interacting micelles, such effects could be assigned to an increasing micellar connectivity and to a stabilization of the water/AOT interface. From an inspection of Fig. 4, we can observe that a break point is also observed in the behavior of ε_0 and τ, at $\phi_V^* \cong 0.32$.

Fig. 4 Dependence of the permittivity at zero frequency (circles) and of the mean relaxation time (squares) upon the volume fraction of the dispersed phase at 25 °C

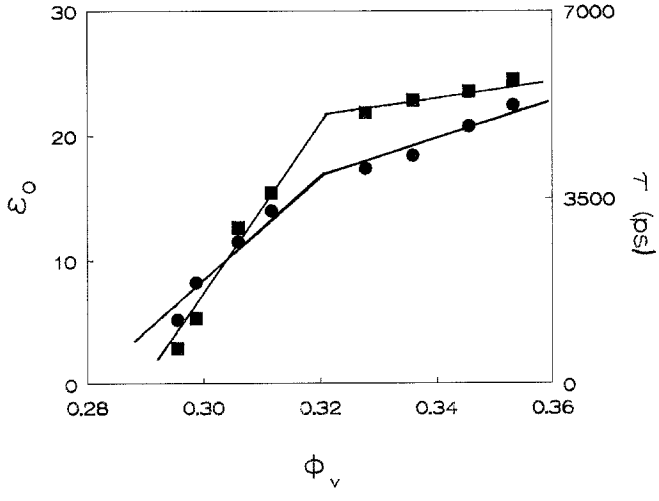

When the ultrasonic velocity data are compared with the hypersonic ones an almost constant value of the sound velocity is revealed for all the samples. Also, the normalized hypersonic absorption data appear to be almost frequency independent. This means that by the Brillouin experiment we are observing the tails of the relaxation processes taking place in our system: every dynamical process giving contributions to the acoustic energy losses takes place on a time scale longer than 10^{-9} s. This is confirmed by the abrupt increase, at low frequency, of the normalized ultrasonic absorption that gives an indication of the existence of same dynamical process taking place in the 10^{-5} s time scale. We tried to obtain the same information about the relaxation frequency by fitting the data with a single relaxation law:

$$\frac{\alpha}{\nu^2} = \frac{N}{1 + \left(\frac{\nu}{\nu_c}\right)^2} + M , \tag{4}$$

where N, ν_c and M are the strength of the relaxation, the relaxation frequency and the relaxed value of the absorption, respectively. The relaxation frequency, which turns out to be about 440 KHz in the gelatin free microemulsion, continuously decreases down to a value of about 160 KHz (at the maximum explored gelatin content) on addition of gelatin. In Fig. 5 we report, as an example, the frequency dependence of the normalized absorption for three different values of the gelatin content. Continuous lines in the same figure represent the results of the fitting procedure with Eq. (4). Although the assumption of a single relaxation process is a crude approximation, the obtained behavior of the relaxation frequency agrees with the hypothesis that the presence of the gelatin molecules induces the existence of a more *rigid* local structural arrangement. The same indication comes from the hypersonic velocity that shows a trend towards a slight increase with the gelatin content (see Fig. 6). In order to obtain additional information about the structural evolution, we calculated the concentration dependence of the adiabatic compressibility by

$$\chi_S = \frac{1}{V}\left(\frac{\partial V}{\partial P}\right)_S = \frac{1}{\rho v^2} . \tag{5}$$

After this, we calculated the contribution of the dispersed phase to the adiabatic compressibility by weighted subtraction of the *n*-heptane contribution. The results are reported in Fig. 7. Also, the compressibility data show a change of the slope, with the tendency to flatten, above a critical value of the volume fraction ($\phi_V^* \cong 0.34$). This suggests the establishment of a lower density local structure when the gelatin content reaches a critical value ($\cong$ 7.5% by weight).

In summary, the following picture can be drawn for the structural evolution of the system after addition of gelatin:

i) When gelatin is added to the heptane/AOT/water system, the gelatin molecules are entrapped within the water pools of the reverse micelles. As a consequence the structure of the micelles is changed (size and density increase and, probably, also the shape is changed).

ii) The micelles begin to interact giving rise to a *rigid* solid-like local structure that coexists with a bulk continuous phase in which gelatin-free micelles are dispersed.

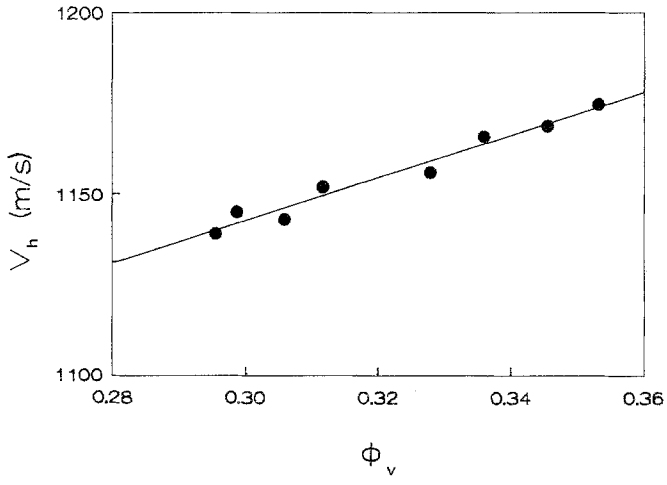

Fig. 6 Dependence of the hypersonic velocity upon the volume fraction of the dispersed phase at 25 °C

Fig. 5 Normalized acoustic absorption for water/AOT/*n*-heptane microemulsions as a function of the frequency. Data at 25 °C are reported for different gelatin contents: gelatin free microemulsions (rhombuses), 7.4% (triangles), 11.3% (circles). Data from pure *n*-heptane (crosses) are reported for comparison. Continuous lines represent the fitting results with Eq. (4)

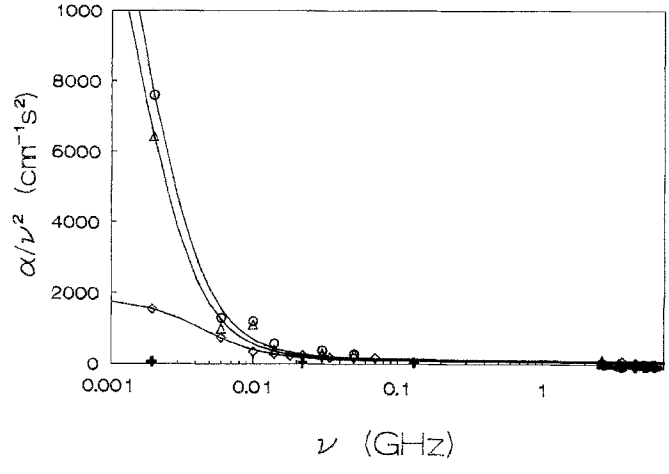

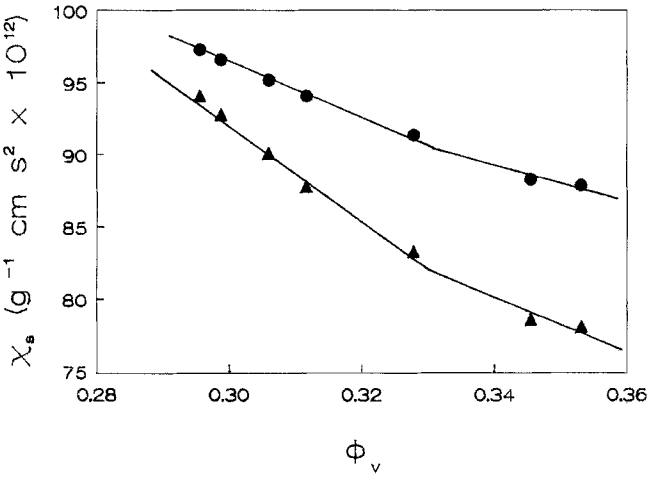

Fig. 7 Dependence of the adiabatic compressibility (circles) and of the micellar adiabatic compressibility (triangles) upon the volume fraction of the dispersed phase at 25 °C

iii) At a critical gelatin content, the *rigid* solid-like local structures percolate giving rise to an *infinite* network.

iv) Further addition of gelatin involves some structural modification of the elementary units (*rod-like* micelles?). Such a situation is well mapped by the density and adiabatic compressibility data, that give strong indication for a structural evolution towards a more expanded but more rigid gel network.

v) Our data appear to be consistent with the small-angle neutron scattering results obtained by Atkinson and coworkers [11] that hypothesized the existence of a rigid network of gelatin–water rods coexisting with microemulsion droplets at the gelatin point.

vi) Our data give strong evidence for additional structural evolution at the higher gelatin contents, which reflect the existence of two distinct regimes with different scaling laws.

References

1. Van Dik MA, Casteleijn G, Joosten JGH, Levin YK (1986) J Chem Phys 85:626
2. D'Aprano A, D'Arrigo G, Paparelli A, Goffredi M, Turco-Liveri V (1993) J Phys Chem 97:3614
3. Lagues M (1979) J Phys (Paris) Lett 40:L-331
4. Safran SA, Webman I, Grest GS (1985) Phys Rev A 32:506
5. Goffredi M, Turco-Liveri V, Vassallo G (1993) J Solution Chem 22:941
6. Haering G, Luisi PL (1986) J Phys Chem 90:5892
7. Luisi PL, Scartazzini R, Haering G, Schurtenberger P (1990) Colloid Polym Sci 268:356
8. Eagland O, Pilling G, Wheeler G (1974) Faraday Discuss Chem Soc 57:181
9. Eastoe J, Fragneto G, Robinson BH, Towey TF, Heenen RH, Leng FJ (1992) J Chem Soc Faraday Trans I 88:461
10. Quellet C, Eicke HF, Sager W (1991) J Phys Chem 95:5642
11. Atkinson PJ, Grimson MJ, Heenan RH, Howe AM, Robinson BH (1989) J Chem Soc Chem Commun 1807
12. D'Aprano A, Lizzio A, Turco-Liveri V (1987) J Phys Chem 91:4749
13. D'Aprano A, Donato DI, Turco-Liveri V (1990) J Sol Chem 19:711
14. Grolier JP, Inglese A, Roux AH, Wilhem E (1981) Ber Bunsenges. Phys Chem 85:768
15. Riddick JA, Bunger WB (1970) In: Waissberger A (Ed) Organic Solvents, Wiley: New York
16. La Manna G, Turco-Liveri V, Aliotta F, Fontanella ME, Milgliardo P (1993) Colloid and Polym Sci 271:1172
17. See, e.g.: Boon JP, Yip S (1980) In: Molecular Hydrodynamics; MGraw-Hill: New York
18. D'Aprano A, D'Arrigo G, Goffredi M, Paparelli A, Turco-Liveri V (1991) J Chem Phys 95:1304